

Bio-nanocomposite Photoelectrode Composed of the Bacteria Photosynthetic Reaction Center Entrapped on a Nanocrystalline TiO₂ Matrix

Yidong Lu ¹, Yuan Liu ², Jingjing Xu ¹, Chunhe Xu ², Baohong Liu ¹ and Jilie Kong ^{1,*}

¹ Department of Chemistry, Fudan University, Shanghai 200433, P. R. China

² Shanghai Institute of Plant Physiology & Ecology, Shanghai Institute for Biological Sciences, Chinese Academy of Science, Shanghai 200032, P. R. China

* Corresponding author. E-mail: jlkong@fudan.edu.cn

Received: 28 May 2004 / Accepted: 1 November 2004 / Published: 4 May 2005

Abstract: A new kind of bio-nanocomposite photoelectrode was fabricated through direct immobilization of the bacterial photosynthetic reaction center (RC) proteins on a nanocrystalline TiO₂ matrix prepared by anodic electrodeposition. The near-infrared (NIR)-visible absorption and fluorescence emission spectra displayed that structure and activity of the RC remained unaltered on the nano-TiO₂ film surface. High efficient light-harvesting of the NIR light energy by RC contributed to the distinct enhancement of the photoelectric conversion on such nanoporous matrix, which would provide a new strategy to develop versatile biomimic energy convertors or photoelectric sensors.

Keywords: Photosynthetic reaction center, nanocrystalline TiO₂, photoelectric, light-harvesting

1. Introduction

Construction and application of dye-sensitized nano-structured semiconductors have achieved considerable progress in the energy conversion efficiency improvement of artificial solar cells [1,2]. Recently, increasing concern has been evoked to improve the photoelectric conversion in the red to near-infrared (NIR) region, but few achievements were acquired at wavelength above 600 nm mainly due to the intricate design and fabrication of a high efficient NIR light-harvesting dye. Since bacterial photosynthetic reaction center (RC) was reported as a functional protein isolated from purple bacteria *Rb. Sphaeroides* with very high quantum efficiency (*ca.* 100%) of the photo-induced charge separation

in the red to NIR region [3, 4], it has been of great interests to construct a photoelectrode through modification of RC onto a specific matrix. In our previous work, multilayered self-assembly [5] and low-temperature Al_2O_3 sol-gel [6] techniques have been employed to fabricate well-defined RC photoelectrodes with obvious photoelectric responses observed in the NIR region. With the aim at further enhancing the photoelectric responses of RC-based photoelectrodes, it is conceivable to make RC serve as a dye to photosensitize the semiconductors that have feeble light absorption at relative long wavelength region for their wide band gaps.

In this work, RC-sensitized nanocrystalline TiO_2 photoelectrodes were fabricated through direct immobilization of the proteins on the matrix prepared by anodic electrodeposition. The photoelectric properties of such bio-photovoltaic apparatus based on the RC/ TiO_2 composite film showed high efficient NIR light-harvesting capability, which made it possible to develop novel biomimic devices.

2. Experimental

Reagents, Apparatus and Procedures

Preparation of the RC/ TiO_2 bio-nanocomposite film

Nanocrystalline TiO_2 was prepared on the ITO glass ($25 \Omega \text{ sq}^{-1}$, area = 2.5 cm^2) by anodic oxidative hydrolysis of TiCl_3 [7]. RC prepared from the photosynthetic bacterium RS601 (one of *Rb. Sphaeroides* strain) was separated and purified as described previously [8]. Protein immobilization was achieved by immersing the TiO_2 films (1.5 cm^2) in the RC solution (at 4°C) for 2 ~ 3 days. The RC solution was composed of $0.5 \sim 4 \mu\text{M}$ RC and the pH 8.0 Tris-HCl buffer consisting of 50 mM Tris (hydroxymethyl) aminomethane and 50 mM KCl. Prior to all measurements, the films were rinsed and kept in buffer solution.

Characterization of the TiO_2 and RC/ TiO_2 composite film

X-ray diffraction (XRD) patterns were recorded with a Bruker D4 diffractometer with Cu $K\alpha$ radiation. Scanning electron micrograph (SEM) experiments were conducted on a JSM-840 microscope. NIR-visible absorption spectra and fluorescence emission spectra were obtained by using a SM-240 CCD spectrophotometer (CVI spectral instruments, Putnam, CT, USA) and a SM-300 luminescence spectrometer (CVI spectral instruments, Putnam, CT, USA) at room temperature, respectively.

Measurement of the photoelectric responses

Photoelectric responses were measured by using the TiO_2 or RC/ TiO_2 films based on ITO glass as the working electrodes, a platinum wire as the counter electrode, and a Ag/AgCl electrode as the reference in a self-made quartz cell filled with 20 mL Tris-HCl buffer solution containing 8 mM sodium dithionite (pH 8.0). The area of the quartz window was estimated to be 1.0 cm^2 . All experimental solutions were deoxygenated by bubbling nitrogen through them for 30 minutes before

measurements. Photocurrent tests were carried out in a shielding box by illuminating the working electrode with a 20 W incandescent lamp. Incident light intensity (I_{inc}) on the external surface of the cell was 5 mW cm^{-2} measured with a CCD detector (SM-240). A filter ($\lambda > 600 \text{ nm}$) was applied or not and the intensity of the output through the filter was measured to be 0.1 mW cm^{-2} . The photoelectric signals were recorded by a CHI-660A electrochemical workstation (CHI Instrument Co., USA). The electrode potential was set at the open-circuit voltage ($\sim -0.15 \text{ V}$ for the bare TiO_2 film and $\sim -0.1 \text{ V}$ for the RC/ TiO_2 film) before measuring the short-circuit photocurrent (I_{sc}). The background dark current was less than 10 nA cm^{-2} .

3. Results and discussion

No distinct diffraction peaks found for the as-made hydrated material indicates the amorphous structure of the TiO_2 film prepared by the anodic electrodeposition. After it was annealed at 450°C for 1.5 h, the high-angle XRD pattern corresponds to the anatase phase of the material (Figure 1). SEM of a ca. 500-nm-thick film consisting of the nanocrystalline TiO_2 particles with grain size ranging from 30-70 nm is shown in Figure 1 inset. The porosity derived from the intercrystalline voids of the TiO_2 film results in a relatively high surface area in favor of dye adsorption [1].

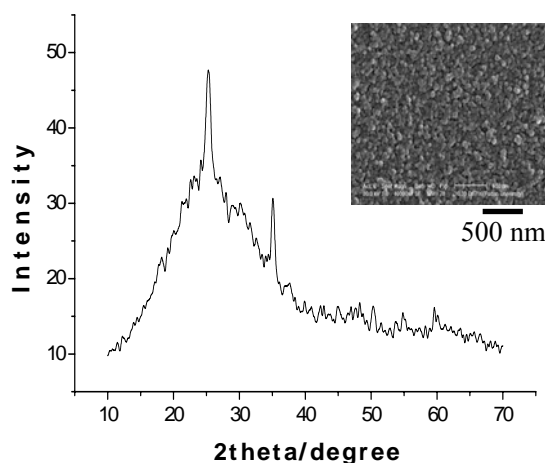


Figure 1. XRD pattern of calcined TiO_2 film prepared by anodic electrodeposition. Inset shows the SEM image of the nanocrystalline TiO_2 film.

The successful entrapment of RC on the surface of nanocrystalline TiO_2 films was proved by the steady NIR-visible absorption and fluorescence emission spectra that give a very useful functional and conformational probe of the photosynthetic proteins. Fig. 2A presents the steady NIR-visible absorption of RC in pH 8.0 Tris-HCl buffer and on the nanocrystalline TiO_2 film. RC (RS601) shows three major absorption peaks at 760, 802 and 870 nm, which correspond predominantly to the Q_y transition for bacteriopheophytin (Bphe), bacteriochlorophyll (BChl) and P (a BChl dimer, also namely P870) respectively [9]. Since photo-induced charge separation can form rapidly upon direct excitation of P or by energy transfer from other pigments [3,4], the high-efficient NIR light harvesting capability of RC may benefit to the photosensitization of the nanocrystalline TiO_2 . Obviously, there is no distinct difference between the two spectrums, which displays that the native status is remained for

RC adsorbed on the TiO₂ matrix. Fig 2B gives the steady fluorescence emission spectra of the RC-free nanocrystalline TiO₂ film and the RC/TiO₂ composite film. Since nanocrystalline TiO₂ film has no luminescence peak in such experimental condition, the fluorescence peak centered at ~ 870 nm can be strongly attributed to the specific emission from P because a high quantum yield of energy transfer from BChl (actinic wavelength at 800 nm) to P was reported [10]. The fluorescence emission of RC modified nanocrystalline TiO₂ film also suggests the well-remained native activity of the photosynthetic proteins.

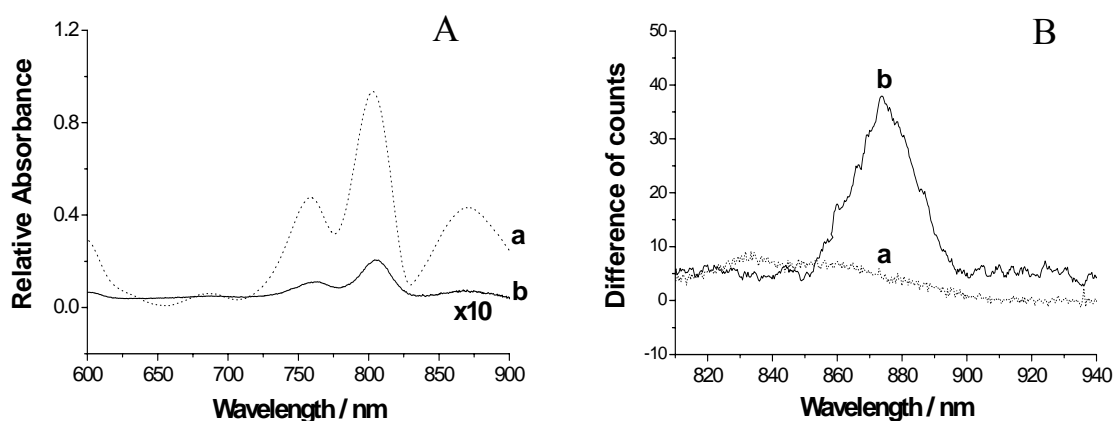


Figure 2. Steady absorption spectra and fluorescence emission spectra of the RC/TiO₂ composite film. (A) NIR-visible absorption spectra of 4 μ M RC in the pH 8.0 Tris-HCl buffer (a, dotted line) and the RC/ TiO₂ film (b, solid line). Absorption of the bare TiO₂ film was subtracted as background. (B) Fluorescence emission spectra of the RC-free TiO₂ film (a, dotted line) and the RC/TiO₂ film (b, solid line) at 293 K, excited at 800 nm and detected at 870 nm.

Figure 3A shows the representative photoelectric responses of the RC/TiO₂ films irradiated with a 20 W incandescent lamp and a filter ($\lambda > 600$ nm, $I_{\text{inc}} = 0.1$ mW cm⁻²). For any RC-free TiO₂ films, no obvious short-circuit photocurrent ($I_{\text{sc}} < 10$ nA cm⁻²) is observed because of its rather feeble light absorption in NIR region. While for all the electrodes immobilized with RC, obvious reproducible anodic photocurrents ($I_{\text{sc}} \sim 120$ nA cm⁻²) are observed immediately when the composite films are illuminated, which strongly indicates that the generated I_{sc} is dominated by the existence of RC. Meanwhile, well-defined I_{sc} derived from the photoelectrode also indicates the high activity of RC entrapped on these nanocrystalline TiO₂ films. The effective perception and harvest of NIR light even at low intensity make the RC be a promising candidate of various artificial bioelectronic or biophotovoltaic devices.

Figure 3B shows the typical photoelectric responses of the RC/TiO₂ films upon illumination with a 20 W incandescent lamp with a light intensity of 5 mW cm⁻². In such cases, TiO₂ and RC absorb different wavelength parts of the light and the electrons in ground state were excited to the conduction band (Cb) of TiO₂ and P* in RC, respectively. The I_{sc} observed for RC/TiO₂ film was 8 μ A cm⁻², which is about two times larger than that for RC-free TiO₂ film (4 μ A cm⁻²). The open-circuit photovoltage measured ($V_{\text{oc}} \sim 30$ mV) is nearly 10 times larger than the RC/Al₂O₃ sol-gel film reported previously [6]

in the same light intensity. Apparently, the combination of RC with nanocrystalline TiO₂ fully enhances the integral light-to-electric conversion efficiency of the photoelectrode.

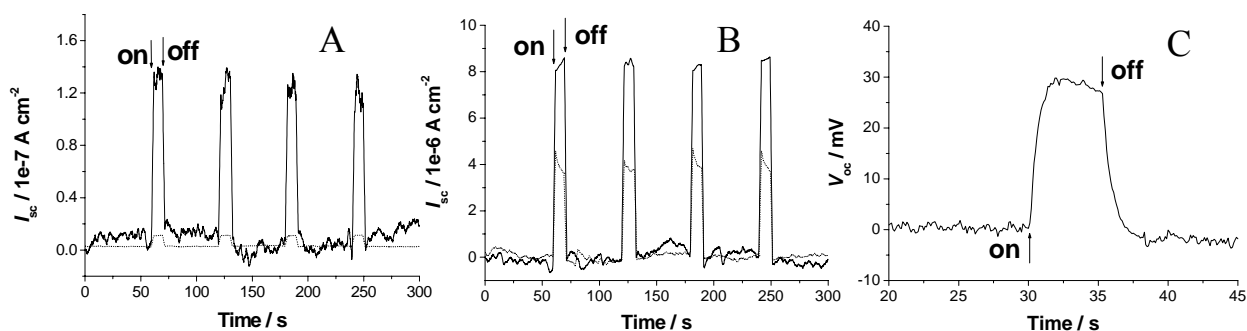


Figure 3. Short-circuit photocurrent (I_{sc}) responses of the RC-free TiO₂ film (a, dotted line) and the RC/TiO₂ film (b, solid line) in the pH 8.0 Tris-HCl buffer containing 8 mM sodium dithionite illuminated with an 20 W incandescent lamp coupled with a filter (A, $I_{inc} = 0.1$ mW cm^{-2}) or not (B, $I_{inc} = 5$ mW cm^{-2}). (C), The open-circuit photovoltage (V_{oc}) responses of the RC/TiO₂ film ($I_{inc} = 5$ mW cm^{-2}).

The reasonable photoelectric conversion process is shown in Figure 4. In RC, the redox potential of light-initiated primary electron donor P is about 0.5 V (vs. standard hydrogen electrode, SHE) [11, 12]. The band gap between the ground state and the excited state of P was reported about 1.1~1.3 eV [13]. When the RC/TiO₂ composite film is illuminated by photons with energy exceeding the band gap of RC, the electrons from the light-induced P* quickly inject the Cb of TiO₂. The photo-generated negative charge carriers can effectively transfer due to the matching energy level of TiO₂ and RC. On the other hand, the simultaneously generated positive holes (P⁺) congregate at the interface between the composite film and the electrolytes to react with the sodium dithionite. High efficient light-harvesting capability of the NIR light energy by RC compensates the negligible light absorption of TiO₂ at long wavelength region, which enables the derived composite films to capture the light energy effectively.

Proton uptake upon the photo reduction of the secondary quinone (Q_B) in RC is a key step in establishment of proton-electrochemical potential, the driving force for ATP formation [14]. The combination of Q_B with H⁺ features an irreversible process in isolated RC, which might somewhat hamper the light-induced charge separation of the RC/TiO₂ composite film. On the other hand, the net surface charge of RC changes from the positive to the negative as the pH of the electrolytes become higher than the isoelectric point of RC (about 7 ~ 8). Since TiO₂ matrix also has a negative surface charge in this pH region, it is considered that the stability of the RC/TiO₂ composite film would be destroyed. In view of the two factors, the optimal pH range for the I_{sc} generation of RC at $\lambda > 600$ nm apparently exists in the neutral pH region, as shown in figure 5A. Figure 5B depicts the relationship between the I_{sc} measured at $\lambda > 600$ nm with the applied bias in pH 8.0 Tris-HCl buffer. Electrode potential is an important factor affecting the photoelectric performance of a photoelectrode. For RC, the applied bias deeply influences the sequence of photo-induced electron transfer between the electron donors and acceptors inside the protein [15] and thus the photoelectric responses of the

RC/TiO₂ film. The maximal I_{sc} observed was obtained at -0.3 V, which is similar to the result for the RC/Al₂O₃ sol-gel film and RC multi-SAMs reported previously [5,6].

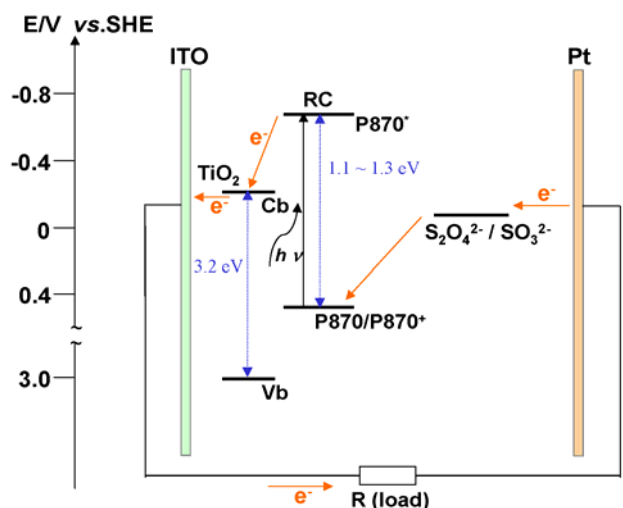


Figure 4. Operation of the RC-sensitized nanocrystalline TiO₂ biophotovoltaic cell. The photoanode is RC/TiO₂ film and the counter-electrode is Pt. The electrolyte is Tris-HCl buffer containing 8 mM sodium dithionite (pH 8.0). P870: bacteriochlorophyll dimer, the primary donor. Cb: conduction band. Vb: valence band.

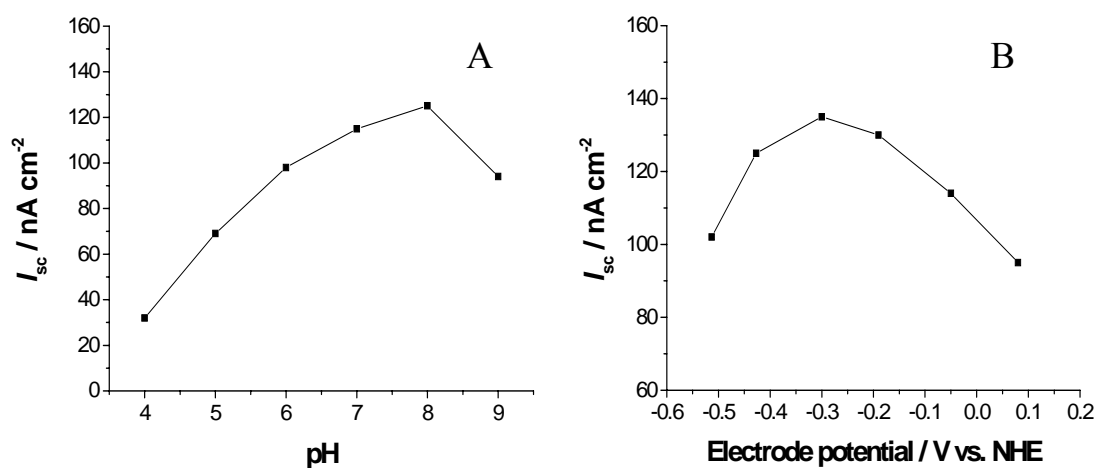


Figure 5. The effects of pH and electrode potential on the photocurrent responses for the TiO₂/RC film at the wavelength of incident light $\lambda > 600$ nm ($I_{inc} = 0.1$ mW cm⁻²). (A) Relationship between the I_{sc} of the RC/TiO₂ film with the pH of the electrolyte. (B) Relationship between the I_{sc} of the RC/TiO₂ film with the electrode bias applied.

4. Conclusions

Bacterial photosynthetic proteins (RC) from *Rb. Sphaeroides* strain RS601 were successfully entrapped on a nanocrystalline TiO₂ film prepared by anodic electrodeposition. The NIR-visible absorption and fluorescence emission spectra displayed that the structure and activity of RC remained unaltered on the surface of TiO₂ film. The effects of the pH and applied bias on the photocurrent performance were investigated. The obviously enhanced photoelectric responses in the red to NIR region were observed for the RC-sensitized nanocrystalline TiO₂. Such strategy of fabricating photosynthetic proteins onto specific matrix provides an alternative way to probe the photo-induced electron transfer of photosensitive chromophores contained composite films. High sensitive and efficient NIR light harvest of RC was achieved on the nano-semiconductor electrode, which opens a new perspective to develop versatile biophotovoltaic converters or sensors.

Acknowledgements

This work was supported by NSFC of China (20335040, 20475012), Shanghai Photo- & Nano-project (011661073, 0244nm029, 0452nm003) and SKLECC.

References and Notes

1. Gratzel, M. Photoelectrochemical cells. *Nature* **2001**, *414*, 338-344.
2. Gratzel, M. Dye-sensitized solar cells. *J. Photochem. Photobiol. C: Photochem Review.* **2003**, *4*, 145-153.
3. Feher, G.; Allen, J. P.; Okamura, M. Y.; Rees, D. C. Structure and function of bacterial photosynthetic reaction centers. *Nature* **1989**, *339*, 111-116.
4. Kirmaier, C.; Gaul, D.; Debey, R.; Holten, D.; Schenck, C. C. Charge Separation in a reaction center incorporating bacteriochlorophyll for photoactive bacteriopheophytin. *Science* **1991**, *251*, 922-927.
5. Zhao, J.; Liu, B.; Zhou, Y.; Xu, C.; Kong, J. Photoelectric conversion of photosynthetic reaction center in multilayered films fabricated by layer-by-layer assembly. *J. Electrochim. Acta.* **2002**, *47*, 2013-2017.
6. Zhao, J.; Ma, N.; Liu, B.; Zhou, Y.; Xu, C.; Kong, J. Photoelectrochemistry of photosynthetic reaction centers embedded in Al₂O₃ gel. *J. Photochem. Photobiol. A:Chem.* **2002**, *152*, 53-60.
7. Kavan, L.; Regan, B. O.; Kay, A.; Gratzel, M. Preparation of TiO₂ (anatase) film on electrode by anodic oxidative hydrolysis of TiCl₃. *J. Electroanal. Chem.* **1993**, *346*, 291-307
8. Zeng, X.; Yu, H.; Wu, Y.; Wu, M.; Wei, J.; Shong, H.; Xu, C. *Acta. Biochim. Biophys. Sinica.* **1997**, *29*, 46-52.
9. Arnett, D. C.; Moser, C. C.; Dutton, P. L.; Scherer, N. F. The first events in photosynthesis: Electronic coupling and energy transfer dynamics in the photosynthetic reaction center from *Rhodobacter sphaeroides*. *J. Phys. Chem. B.* **1999**, *103*, 2014-2032.
10. Wright, C.A.; Clayton, R.K. The absolute quantum efficiency of bacteriochlorophyll photooxidation in reaction centres of *Rhodospseudomonas sphaeroides*, *Biochim. Biophys. Acta.*, **1973**, *333*, 246-260.

11. Kong, J.; Lu, Z.; Lvov, Y. M.; Desamero, R. Z. B.; Frank, H. A.; and Rusling, J. F. Direct electrochemistry of cofactor redox sites in a bacterial photosynthetic reaction center protein. *J. Am. Chem. Soc.* **1998**, *120*, 7371-7372.
12. Ivancich, A.; Artz, K.; Williams, J. C.; Allen, J. P.; Mattioli, T. A. Effects of hydrogen bonds on the redox potential and electronic structure of the bacterial primary electron donor. *Biochemistry* **1998**, *37*, 11812-11820.
13. Moser, C.C.; Sension, R. J.; Szarka, A. Z.; Repinec, S.T.; Hochstrasser, R.M.; Dutton, P.L. Initial Charge Separation Kinetics of bacterial photosynthetic reaction centers in oriented Langmuire-Blodgett-films in an applied electric field. *Chem. Phys.* **1995**, *197*, 343-354.
14. Okamura, M. Y.; Feher, G. Proton-Transfer in reaction centers from photosynthetic bacteria. *Annu. Rev. Biochem.* **1992**, *61*, 861-896.
15. Zhao, J., Zhou, Y.; Liu, B.; Xu, C.; Kong, J. Differentiating the orientations of photosynthetic reaction centers on Au electrodes linked by different bifunctional reagents. *Biosens. Bioelectron.* **2002**, *17*, 711-718.